Publishing Excellence Inspiring Progress
ARISTON PUBLICATIONS
CompSci & AI Advances
ISSN: 3066-3806 www.aristonpubs.com/journal/compsci-ai-advancess https://doi.org/10.69626/cai.2026.0308

RESEARCH ARTICLE

Content – Based Image Retrieval Tool for Grape and Pomegranate Disease Detection using Colour, Texture and Shape Features: Development and Field Validation

Bhagawan N. Kadlag*, Dhananjay N. Kadlag, Anil G. Khairnar, Chandrakant G. Dighavkar, Arun V. Patil

ABSTRACT: Grape (*Vitis vinifera L.*) and pomegranate (*Punica granatum L.*) are high-value export crops of Maharashtra, India, and fungal and bacterial diseases of their leaves and fruits reduce both yield and export quality. Field diagnosis still relies on slow visual inspection by experts. This study developed a content-based image retrieval (CBIR) tool in MATLAB that identifies diseases in grape and pomegranate images and shows the user the most similar confirmed cases from its image database. Images are enhanced and converted to the HSI and CIELAB colour spaces. Diseased regions are isolated by thresholding, Canny edge detection and K-means clustering, and colour-histogram, grey-level co-occurrence matrix (GLCM) texture and shape features form the image descriptor. Similar images are retrieved by Euclidean distance, and support vector machine (SVM), artificial neural network (ANN), k-nearest neighbour (KNN) and naive Bayes (NB) classifiers assign the disease class. The image collection holds 35,000 images (25,000 grape and 10,000 pomegranate) from public repositories and the authors' own field collection in Nashik district; 1,000 images train the classifiers and the remaining 34,000 form the retrieval database. On this collection the tool reached 98.2% accuracy and 97.5% sensitivity for grape and 98.8% accuracy and 97.9% sensitivity for pomegranate. On an independent field-validation set of 500 samples from 100 farmers, with diagnoses confirmed by an agricultural expert and by laboratory analysis, it classified 490 samples correctly (98.0% accuracy) with 97.2% sensitivity. The tool needs no graphics processor, and each diagnosis is shown beside the confirmed images it matched.

Keywords: : Content-Based Image Retrieval; Plant Disease Detection; Grape; Pomegranate; Grey-Level Co-Occurrence Matrix; K-Means Segmentation; Support Vector Machine; Precision Agriculture.

Received: 20 October 2026; Revised: 02 November 2026; Accepted: 04 November 2026; Published Online: 10 November 2026

1. INTRODUCTION

Grape and pomegranate are among the most valuable fruit crops of Maharashtra, India. The state leads national grape production, and Nashik district contributes about 73% of the state's grape production and around 82% of grape exports, which go mainly to the Netherlands, Bangladesh, Russia, the United Kingdom and the United Arab Emirates [1]. India grew pomegranate on 278,000 ha with a production of 3.19 million t in 2020–21, and Maharashtra cultivates about 162,000 ha of the crop with a production of 1.75 million t [2]. Both crops are grown for demanding export markets, so lower yields and blemished fruit translate directly into lost income for growers.

Plant diseases are a major threat to crop production and food security [3]. Grape leaves and bunches are attacked by diseases such as downy mildew, powdery mildew, black rot, Esca (black measles) and leaf blight (Isariopsis leaf spot). In pomegranate, bacterial blight caused by Xanthomonas axonopodis pv. punicae affects all aerial parts of the plant except

Research Center in Electronic Science, MGV's L. V. H. Arts, Science and Commerce College, Panchavati, Nashik 422003, Maharashtra, India

*Author to whom correspondence should be addressed: kadlag1985@gmail.com (B. Kadlag)

© Ariston Publications 2026. All rights reserved.

the flowers [4], while anthracnose, Cercospora fruit spot and Alternaria fruit spot blemish the fruit. Growers usually diagnose these diseases by eye or by consulting an expert. Visual diagnosis is slow, depends on scarce expertise and is subjective [5], and a late or wrong diagnosis leads to poorly targeted sprays that raise production costs.

Image-based diagnosis offers a faster alternative. Classical pipelines segment the lesion, extract colour, texture and shape features and pass them to a statistical classifier [6, 7]. Deep convolutional neural networks (CNNs) now dominate the field: Mohanty et al. reached 99.35% accuracy on 54,306 PlantVillage leaf images [8], and Ferentinos reported a 99.53% success rate on 87,848 images in 58 plant–disease classes [9]. Their accuracy, however, falls sharply when images differ from the training conditions; the model of Mohanty et al. reached only about 31% on images collected from online sources [8]. Deep networks also need large and diverse labelled datasets [10], are usually trained on graphics processors, and return a class label without showing the evidence behind it. Opaque outputs of this kind are difficult to trust in high-stakes decisions [11], such as whether to spray an export orchard.

Content-based image retrieval (CBIR) addresses this transparency problem. A CBIR system describes each image by its visual content (colour, texture and shape) and returns the database images closest to a query [12]. In disease diagnosis the retrieved images are confirmed cases, so the user sees the predicted disease together with its most similar reference images and can judge the match. CBIR descriptors are also inexpensive to compute and run on an ordinary computer. Our earlier study applied CBIR to disease detection in grape and pomegranate [13]. This paper develops that approach into a complete software tool and evaluates it on a large image collection and in farmers' fields.

The main contributions of this work are:

- A CBIR tool with a graphical user interface (GUI), built in MATLAB, that combines colour-histogram, grey-level co-occurrence matrix (GLCM) texture and shape features with Euclidean-distance retrieval and four classifiers (SVM, ANN, KNN and NB) to identify diseases of both grape and pomegranate.
- A collection of 35,000 images (25,000 grape and 10,000 pomegranate) that combines public repositories with field images from Nashik district whose labels were confirmed by an expert and by laboratory analysis.
- An independent field validation on 500 samples collected from 100 farmers, in addition to evaluation on the image collection.
- An explainable output in which every prediction is displayed with the infected region and the most similar confirmed images.

Section 2 reviews related work, Section 3 describes the materials and methods, Section 4 presents the results, Section 5 discusses them and Section 6 concludes the paper.

2. RELATED WORK

2.1 Hand-crafted Feature Pipelines

Early image-based systems followed a fixed pipeline of segmentation, feature extraction and classification [6, 7]. Camargo and Smith developed an algorithm that automatically identifies the visual symptoms of plant disease in colour images [14]. Al Bashish et al. combined K-means segmentation with a neural-network classifier to classify leaf diseases [15], and Pujari et al. addressed the image-based detection of fungal diseases in plants [16]. Dubey and Jalal classified apple diseases from colour, texture and shape features [17], the same three feature families used in this work.

For the crops studied here, Padol and Yadav applied a support vector machine (SVM) classifier to grape leaf disease detection [18]. Bhange and Hingoliwala built a web-based tool that extracts colour, morphology and colour-coherence-vector features from pomegranate fruit images, groups them by K-means clustering and labels the fruit as infected or healthy with an SVM; they reported 82% accuracy [19]. Such systems need little training data and run on ordinary computers, but these two crop-specific systems each covered one crop, and hand-crafted features are sensitive to illumination, background and variable symptoms [5].

2.2 Deep Learning

CNNs learn features directly from pixels. Mohanty et al. [8] and Sladojevic et al. [20] showed that CNNs can recognise many diseases from leaf images, and Too et al. found DenseNet-121 the best of several fine-tuned architectures, with 99.75% test accuracy on 38 PlantVillage classes [21]. Ferentinos trained CNNs on 58 plant–disease classes [9], Liu et al. adapted deep CNNs to grape leaf diseases [22], and Kamilaris and Prenafeta-Boldú surveyed the wider use of deep learning in agriculture [23].

© Ariston Publications 2026. All rights reserved.

Table 1. Composition of the image collection and the field-validation set.

Set	Crop and plant part	Disease classes	Source	Images
Image collection	Grape: leaves (public); leaves, stems and fruits (field)	Public: black rot; Esca (black measles); leaf blight (Isariopsis leaf spot); healthy. Field: downy mildew; powdery mildew; black rot; healthy	PlantVillage via Kaggle [24]; authors' field images, Nashik	25,000
Image collection	Pomegranate: fruits (public); leaves, stems and fruits (field)	Public: bacterial blight; anthracnose; Cercospora fruit spot; Alternaria fruit spot; healthy. Field: bacterial blight; anthracnose; fruit rot; healthy	Pakruddin and Hemavathy [25] via Kaggle; authors' field images, Nashik	10,000
Field validation	Grape and pomegranate	Diseases present on the participating farms	100 farmers, Nashik district; expert and laboratory diagnosis	500

Much of this work relies on PlantVillage, an open repository of more than 50,000 expertly curated images of healthy and diseased leaves [24]. Real field images are harder. Singh et al. assembled PlantDoc, 2,598 real-world images of 13 plant species, and showed that training on such images increased classification accuracy by up to 31% [26]. Barbedo identified limited and insufficiently diverse training data as a key factor that limits deep learning for disease recognition [10], and Toda and Okura investigated how CNNs arrive at their diagnoses [27], reflecting a wider concern that these decisions are hard to interpret [11]. For pomegranate, Pakruddin and Hemavathy released 5,099 fruit images in five classes collected from farms in Karnataka [25].

2.3 Image Retrieval for Plant Disease

CBIR is well established in computer vision [12] but has seldom been applied to plant disease. Patil and Kumar built a CBIR system for diseased soybean leaves that combined HSV colour histograms, SIFT shape features and a new Local Gray Gabor Pattern texture feature; average retrieval efficiency was 80% for the top five results and 72% for the top ten [28]. Our earlier study applied CBIR to grape and pomegranate [13]. We found no CBIR tool that covers the diseases of both crops, combines retrieval with supervised classifiers and has been validated with samples from farmers' fields. The present work addresses this gap.

3. MATERIALS AND METHODS

3.1 System Overview

The tool works in two phases (Figure 1). In the offline phase every image of the collection is preprocessed and segmented, and its colour, texture and shape features are combined into a labelled feature vector; the vectors of 34,000 images form the retrieval database and those of the other 1,000 images train the classifiers. In the online phase a query image loaded through the GUI passes through the same steps; its feature vector is matched against the database to retrieve the most similar confirmed images, and the trained classifiers predict its disease class. The tool was implemented in MATLAB (MathWorks, Natick, MA, USA) with the Image Processing, Computer Vision, and Statistics and Machine Learning Toolboxes and the MATLAB GUI development tools.

3.2 Image Acquisition and Dataset

The image collection contains 35,000 images: 25,000 of grape and 10,000 of pomegranate (Table 1). Of these, 1,000 images were used to train the classifiers and the remaining 34,000 form the retrieval database. Public images were obtained from Kaggle and other open online repositories. They include grape leaf images from the PlantVillage repository [24] and pomegranate fruit images from the dataset of Pakruddin and Hemavathy [25]. PlantVillage labels its grape disease classes "Black rot", "Esca (Black Measles)" and "Leaf blight (Isariopsis Leaf Spot)"; black measles is the leaf and berry symptom of the Esca disease complex [29], so each paired name denotes a single class. The pomegranate dataset contains healthy fruit and fruit affected by bacterial blight, anthracnose, Cercospora fruit spot and Alternaria fruit spot [25].

Field images of healthy and diseased leaves, stems and fruits were collected by the authors from grape and pomegranate farms in Nashik district in different seasons. They were captured with DSLR cameras under controlled lighting, following a standard protocol that fixed the camera distance, angle, orientation and illumination. Each sample was recorded with its sample number, location, date, suspected disease and environmental conditions. Diagnoses were confirmed by laboratory reports from recognised laboratories, including Vanit Agro Laboratories and Agro Fab Lab, and the images were assigned to disease classes on the basis of these reports. The field-validation set comprises 500 samples collected from the farms of 100 farmers in

© Ariston Publications 2026. All rights reserved.

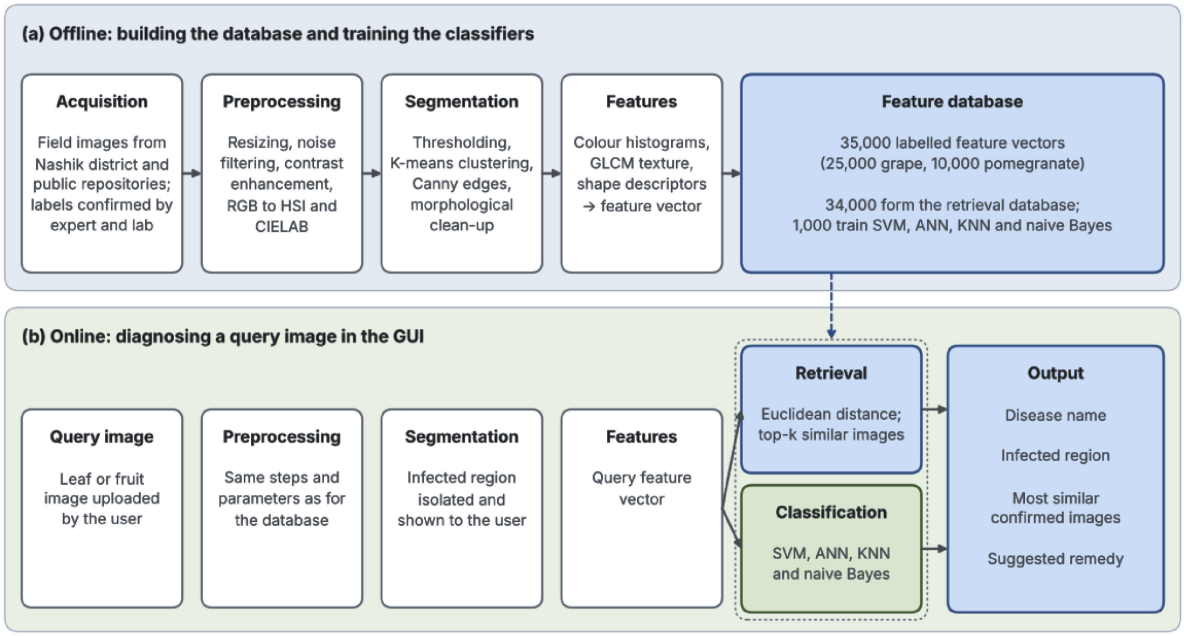


Fig. 1. Architecture of the CBIR tool. (a) Offline phase: images are processed into labeled feature vectors; 34,000 form the retrieval database and 1,000 train the classifiers. (b) Online phase: a query image is processed in the same way, matched against the database and classified. The dashed arrow marks the stored vectors and trained classifiers used at query time. Diagram drawn with the assistance of an AI tool from the authors' description of the system.

Nashik district, independently of the image collection. The diagnosis of each sample was established by an agricultural expert and cross-checked by laboratory analysis, and this confirmed diagnosis served as the reference standard.

3.3 Preprocessing

Images were resized to a common resolution, filtered to suppress noise, contrast-enhanced and normalised, and the background was removed [30]. The RGB images were then converted to the HSI and CIELAB colour spaces, which separate intensity from colour information, are less sensitive to illumination changes than RGB and are closer to human colour perception [30]. For normalised R, G and B values, the HSI components are

$$I = \frac{R+G+B}{3}, \qquad S = 1 - \frac{3\min(R,G,B)}{R+G+B} \tag{1}$$

$$H = \begin{cases} \theta, & B \le G \\ 360^\circ - \theta, & B > G' \end{cases} \tag{2}$$

$$\theta = \cos^{-1}\left[\frac{\frac{1}{2}\left[(R-G)+(R-B)\right]}{\sqrt{(R-G)^2+(R-B)(G-B)}}\right]$$

3.4 Segmentation

Segmentation separates the diseased region from healthy tissue and the background. Grey-level thresholding [31] separates the leaf or fruit from the background, and K-means clustering [32] then groups the pixels by colour so that diseased tissue is separated from healthy tissue. K-means minimises the within-cluster sum of squared distances.

$$J = \sum_{j=1}^{K} \sum_{\mathbf{x}_i \in C_j} \left\| \mathbf{x}_i - \boldsymbol{\mu}_j \right\|^2 \tag{3}$$

where x_i is the colour vector of pixel i, C_j is cluster j, μ_j is its centroid and K is the number of clusters. The Canny detector [33] marks the lesion boundaries, and morphological operations remove small spurious regions and fill holes in the lesion mask.

3.5 Feature Extraction

Each segmented image is described by colour, texture, shape and edge features; colour, texture and shape features have proved complementary in disease classification [17]. Colour. Histograms of the red, green and blue channels [34] and statistical descriptors of the colour channels, such as their mean and standard deviation, describe the colour of the lesion. Texture. The grey-level co-occurrence matrix (GLCM) *P(i,j)* counts how often a pixel

© Ariston Publications 2026. All rights reserved.

of grey level i occurs at a fixed offset from a pixel of grey level j [35]. After normalisation, $p(i,j)=P(i,j)/\sum_{(i,j)}P\ (i,j)$, five texture descriptors are computed:

$$\text{Contrast} = \sum_{i,j}(i-j)^2 p(i,j),$$
$$\text{Energy} = \sum_{i,j} p(i,j)^2 \tag{4}$$

$$\text{Homogeneity} = \sum_{i,j} \frac{p(i,j)}{1+|i-j|},$$
$$\text{Dissimilarity} = \sum_{i,j} |i-j| p(i,j) \tag{5}$$

$$\text{Entropy} = -\sum_{i,j} p(i,j)\log_2 p(i,j) \tag{6}$$

Shape and edges: Shape and morphological descriptors of the segmented lesion, together with the histogram of strong edges produced by the Canny detector, describe the form and boundary structure of the lesions.

The features of each image are concatenated into a single feature vector of length M.

3.6 Similarity Matching and Retrieval

For a query vector q, the tool computes the Euclidean distance to every database vector x [12]:

$$d(\mathbf{q},\mathbf{x}) = \sqrt{\sum_{m=1}^{M}(q_m - x_m)^2} \tag{7}$$

The database images with the smallest distances are returned and displayed with their disease labels, so that the user can compare the query with confirmed cases.

3.7 Classification

Four supervised classifiers were implemented and trained on the labelled feature vectors of the 1,000 training images: an SVM, which finds the maximum-margin boundary between classes [36]; a feed-forward ANN trained by back-propagation [37]; KNN, which assigns the majority class among the nearest database vectors [38]; and NB, which applies Bayes' rule with the features assumed to be conditionally independent given the class [39].

3.8 Graphical User Interface

The tool is operated through a GUI built in MATLAB. Through it the user loads images, runs the analysis, views the retrieved similar images and reads the diagnosis with a suggested remedy, and the result can be saved as a report. Figure 2 shows the comparison screen: the user loads a reference image and a test image, and the tool displays both in colour and in grey scale with the red, green and blue histograms of each, computes their Canny edge maps and reports the result of the comparison. The tool runs on a standard personal computer.

3.9 Evaluation

The tool was evaluated on the image collection and on the independent field-validation set. Accuracy is the proportion of images assigned to the correct class, and sensitivity (recall) is the proportion of positive cases that are correctly identified [40]

$$\text{Accuracy} = \frac{N_{correct}}{N_{total}},$$
$$\text{Sensitivity} = \frac{TP}{TP+FN} \tag{8}$$

where $N_{correct}$ is the number of correctly classified images, N_{total} is the total number of images, TP is the number of true positives and FN is the number of false negatives.

4. RESULTS AND DISCUSSIONS

Table 2 reports the accuracy and sensitivity of the tool on the image collection and on the independent field-validation set. On the collection the tool identified grape diseases with 98.2% accuracy and 97.5% sensitivity, and pomegranate diseases with 98.8% accuracy and 97.9% sensitivity. Of the 500 field samples, whose diagnoses were confirmed by an expert and by laboratory analysis, it classified 490 correctly (98.0% accuracy), with 97.2% sensitivity.

Because the field samples played no part in training the classifiers or in the retrieval database, the field figures are the best estimate of the tool's performance in practice. Field accuracy was 0.2–0.8 percentage points below the collection figures, and field sensitivity 0.3–0.7 points below them. The GUI shows the image features behind each comparison (Figure 2), so the user can check every result.

© Ariston Publications 2026. All rights reserved.

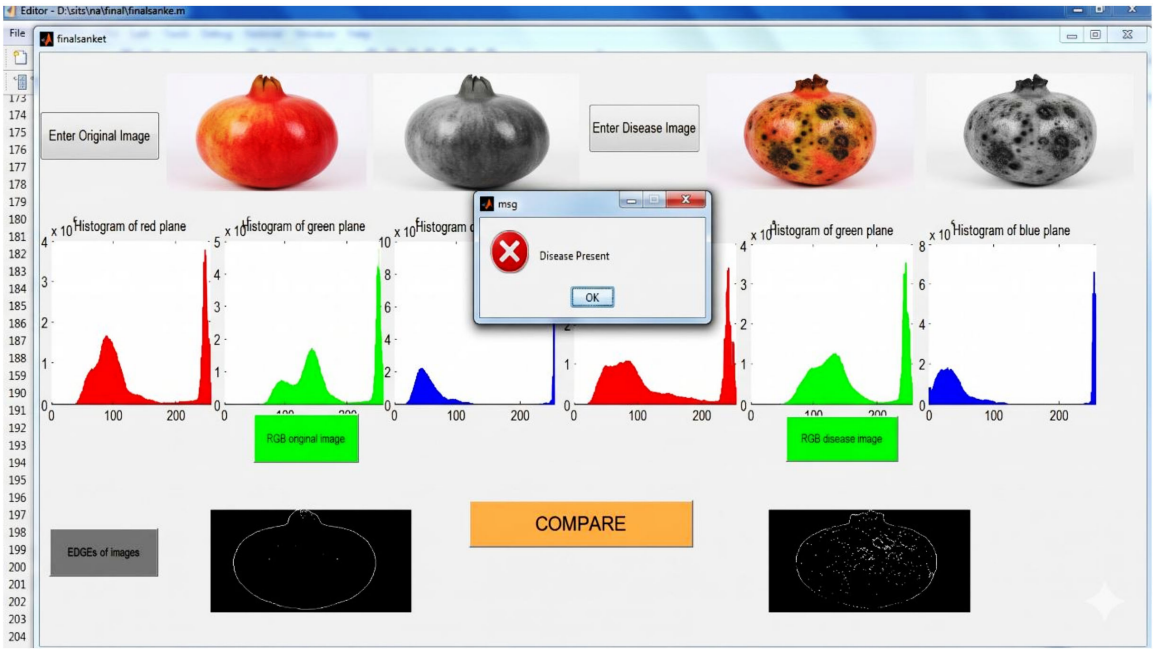


Fig. 2. Comparison screen of the MATLAB GUI. A reference image (left) and a test image (right) are shown in colour and grey scale, with the red, green and blue histograms of each; their Canny edge maps appear below, and the message box gives the result of the comparison.

The tool identified diseases of both crops with close to 98% accuracy on the image collection and kept that level on samples from farmers' fields. The gap between laboratory and field performance is a central weakness of image-based diagnosis: the CNN of Mohanty et al. fell from 99.35% on held-out PlantVillage images to about 31% on images from other sources [8], and Barbedo identified the limited size and diversity of training data as a key cause of such failures [10]. Here the image collection contained field images from the same district, and field accuracy stayed within 1 percentage point of the collection figures. This suggests that adding local field images to the database helps the tool cope with field conditions, although the validation covered a single district.

Table 2. Performance of the CBIR tool.

Evaluation set	Images or samples	Accuracy (%)	Sensitivity (%)
Grape, image collection	25,000	98.2	97.5
Pomegranate, image collection	10,000	98.8	97.9
Field validation, 100 farmers	500	98.0	97.2

Comparisons with published figures need care, because the studies differ in crops, classes, image sources and evaluation protocols. Deep CNNs report 99.35–99.75% on large public image collections [8, 9, 21]; the present tool reaches a similar level on its own database with hand-crafted features and without a graphics processor. Among hand-crafted systems for the same crops, Bhange and Hingoliwala reported 82% accuracy for detecting disease in pomegranate fruit [19]. In the closest CBIR study, Patil and Kumar reported an average retrieval efficiency of 80% for the top five soybean images [28].

The main practical advantage of the retrieval design is transparency. Each prediction is shown with the confirmed images it was matched to, so an extension worker or farmer can check whether the retrieved lesions resemble the query and reject an implausible match. This answers the concern that opaque classifiers are hard to trust in high-stakes decisions [11, 27]. Because colour, texture and shape features are inexpensive to compute, the tool also runs on an ordinary computer, which suits extension offices and diagnostic laboratories.

The study has five limitations. First, the tool recognises only the classes in its database, so a new disease, or a leaf with two diseases, is assigned to the nearest known class. Second, colour and texture features are sensitive to illumination, background and variable symptoms [5], and most public images were captured under more uniform conditions than field photographs. Third, the field validation covered 500 samples from one district, so performance in other regions and seasons remains to be tested. Fourth, this paper reports the performance of the complete tool; a per-class and per-classifier analysis with confusion matrices, a quantitative evaluation of retrieval precision and a comparison with CNNs trained on the same images remain to be done. Fifth, a MATLAB licence is required to run the tool, which limits its use by individual farmers.

 © Ariston Publications 2026. All rights reserved.

5. CONCLUSION

This study developed a CBIR tool in MATLAB that detects diseases of grape and pomegranate from colour, GLCM texture and shape features, retrieves the most similar confirmed images by Euclidean distance and classifies the query with SVM, ANN, KNN and NB classifiers. On a collection of 35,000 images, the tool reached 98.2% accuracy for grape and 98.8% for pomegranate, and it classified 490 of 500 field samples from 100 farmers correctly (98.0% accuracy, 97.2% sensitivity), with diagnoses confirmed by an expert and a laboratory. Because every diagnosis is presented with the confirmed images behind it, the result is transparent to its users, and the tool needs only an ordinary computer.

Future work will (i) report per-class and per-classifier results and retrieval precision, and compare the tool with CNNs trained on the same images, (ii) extend the database to more diseases, seasons and regions, (iii) estimate disease severity from the segmented lesion area, and (iv) port the tool to a mobile application with interfaces in regional languages, so that farmers can use it in the field without a MATLAB license.

DECLARATIONS

Ethical Approval

We affirm that this manuscript is an original work, has not been previously published, and is not currently under consideration for publication in any other journal or conference proceedings. All authors have reviewed and approved the manuscript, and the order of authoR$_{sh}$ip has been mutually agreed upon.

Funding

There are no funding

Availability of Data and Material

The public images are available from the PlantVillage repository [24] and from Mendeley Data [25]. The field images are available from the corresponding author on reasonable request.

Conflicts of Interest

The authors declare that they have no financial or personal interests that could have influenced the research and findings presented in this paper. The authors alone are responsible for the content and writing of this article.

Author's Contributions

All authors equally contributed

Acknowledgements

The authors thank the farmers of Nashik district who provided samples, and Vanit Agro Laboratories and Agro Fab Lab for laboratory analysis

REFERENCES

[1] National Horticulture Board, **n.d.**. Nashik: Grape Capital of India. *Cluster Brochure*, https://www.nhb.gov.in/pdf/NashikBrochure.pdf.

[2] National Horticulture Board, **n.d.**. Solapur Pomegranate: Nature's Goodness in a Fruit. *Cluster Brochure*, https://nhb.gov.in/pdf/SolapurBrochure.pdf.

[3] Strange, R. N.; Scott, P. R., **2005**. Plant disease: A threat to global food security. *Annual Review of Phytopathology*, 43, p.83-116. https://doi.org/bgmj2v.

[4] Sharma, J.; Sharma, K. K.; Kumar, A.; Mondal, K. K.; Thalor, S.; Maity, A.; Gharate, R.; Chinchure, S.; Jadhav, V. T., **2017**. Pomegranate bacterial blight: Symptomatology and rapid inoculation technique for Xanthomonas axonopodis pv. punicae. *Journal of Plant Pathology*, 99, p.109-119.

[5] Barbedo, J. G. A., **2016**. A review on the main challenges in automatic plant disease identification based on visible range images. *Biosystems Engineering*, 144, p.52-60. https://doi.org/f8jspq.

[6] Barbedo, J. G. A., **2013**. Digital image processing techniques for detecting, quantifying and classifying plant diseases. *SpringerPlus*, 2, p.660. https://doi.org/10.1186/2193-1801-2-660.

[7] Kaur, S.; Pandey, S.; Goel, S., **2019**. Plants disease identification and classification through leaf images: A survey. *Archives of Computational Methods in Engineering*, 26, p.507-530. https://doi.org/10.1007/s11831-018-9255-6.

[8] Mohanty, S. P.; Hughes, D. P.; Salathé, M., **2016**. Using deep learning for image-based plant

© Ariston Publications 2026. All rights reserved.

disease detection. *Frontiers in Plant Science*, 7, p.1419. https://doi.org/10.3389/fpls.2016.01419.

[9] Ferentinos, K. P., **2018**. Deep learning models for plant disease detection and diagnosis. *Computers and Electronics in Agriculture*, 145, p.311-318. https://doi.org/10.1016/j.compag.2018.01.009.

[10] Barbedo, J. G. A., **2018**. Factors influencing the use of deep learning for plant disease recognition. *Biosystems Engineering*, 172, p.84-91. https://doi.org/gd3dh2.

[11] Rudin, C., **2019**. Stop explaining black box machine learning models for high stakes decisions and use interpretable models instead. *Nature Machine Intelligence*, 1, p.206-215. https://doi.org/10.1038/s42256-019-0048-x.

[12] Smeulders, A. W. M.; Worring, M.; Santini, S.; Gupta, A.; Jain, R., **2000**. Content-based image retrieval at the end of the early years. *IEEE Transactions on Pattern Analysis and Machine Intelligence*, 22, p.1349-1380. https://doi.org/10.1109/34.895972.

[13] Kadlag, B. N.; Kadlag, D. N.; Dighavkar, C. G.; Patil, A. V., **2023**. Detection of disease in grape and pomegranate plants using content base image retrieval technique. *International Journal of Universal Research and Technology*, 9(5).

[14] Camargo, A.; Smith, J. S., **2009**. An image-processing based algorithm to automatically identify plant disease visual symptoms. *Biosystems Engineering*, 102, p.9-21. https://doi.org/d592jm.

[15] Al Bashish, D.; Braik, M.; Bani-Ahmad, S., **2011**. Detection and classification of leaf diseases using K-means-based segmentation and neural-networks-based classification. *Information Technology Journal*, 10, p.267-275. https://doi.org/10.3923/itj.2011.267.275.

[16] Pujari, J. D.; Yakkundimath, R.; Byadgi, A. S., **2015**. Image processing based detection of fungal diseases in plants. *Procedia Computer Science*, 46, p.1802-1808. https://doi.org/10.1016/j.procs.2015.02.137.

[17] Dubey, S. R.; Jalal, A. S., **2016**. Apple disease classification using color, texture and shape features from images. *Signal, Image and Video Processing*, 10, p.819-826. https://doi.org/10.1007/s11760-015-0821-1.

[18] Padol, P. B.; Yadav, A. A., **2016**. SVM classifier based grape leaf disease detection. , p.175-179. https://doi.org/10.1109/CASP.2016.7746160.

[19] Bhange, M. A.; Hingoliwala, H., **2015**. Smart farming: Pomegranate disease detection using image processing. *Procedia Computer Science*, 58, p.280-288. https://doi.org/10.1016/j.procs.2015.08.022.

[20] Sladojevic, S.; Arsenovic, M.; Anderla, A.; Culibrk, D.; Stefanovic, D., **2016**. Deep neural networks based recognition of plant diseases by leaf image classification. *Computational Intelligence and Neuroscience*, 2016, p.3289801. https://doi.org/10.1155/2016/3289801.

[21] Too, E. C.; Yujian, L.; Njuki, S.; Yingchun, L., **2019**. A comparative study of fine-tuning deep learning models for plant disease identification. *Computers and Electronics in Agriculture*, 161, p.272-279. https://doi.org/10.1016/j.compag.2018.03.032.

[22] Liu, B.; Ding, Z.; Tian, L.; He, D.; Li, S.; Wang, H., **2020**. Grape leaf disease identification using improved deep convolutional neural networks. *Frontiers in Plant Science*, 11, p.1082. https://doi.org/10.3389/fpls.2020.01082.

[23] Kamilaris, A.; Prenafeta-Boldú, F. X., **2018**. Deep learning in agriculture: A survey. *Computers and Electronics in Agriculture*, 147, p.70-90. https://doi.org/10.1016/j.compag.2018.02.016.

[24] Hughes, D. P.; Salathé, M., **2015**. An open access repository of images on plant health to enable the development of mobile disease diagnostics. *arXiv preprint arXiv:1511.08060*. https://doi.org/10.48550/arXiv.1511.08060.

[25] Pakruddin, B.; Hemavathy, R., **2024**. A comprehensive standardized dataset of numerous pomegranate fruit diseases for deep learning. *Data in Brief*, 54, p.110284. https://doi.org/10.1016/j.dib.2024.110284.

[26] Singh, D.; Jain, N.; Jain, P.; Kayal, P.; Kumawat, S.; Batra, N., **2020**. PlantDoc: A dataset for visual plant disease detection. , p.249-253. https://doi.org/10.1145/3371158.3371196.

[27] Toda, Y.; Okura, F., **2019**. How convolutional neural networks diagnose plant disease. *Plant Phenomics*, 2019, p.9237136. https://doi.org/10.34133/2019/9237136.

 © Ariston Publications 2026. All rights reserved.

[28] Patil, J. K.; Kumar, R., **2017**. Analysis of content based image retrieval for plant leaf diseases using color, shape and texture features. *Engineering in Agriculture, Environment and Food*, 10, p.69-78. https://doi.org/10.1016/j.eaef.2016.11.004.

[29] Mugnai, L.; Graniti, A.; Surico, G., **1999**. Esca (black measles) and brown wood-streaking: Two old and elusive diseases of grapevines. *Plant Disease*, 83, p.404-418. https://doi.org/10.1094/PDIS.1999.83.5.404.

[30] Gonzalez, R. C.; Woods, R. E., **2018**. Digital Image Processing. .

[31] Otsu, N., **1979**. A threshold selection method from gray-level histograms. *IEEE Transactions on Systems, Man, and Cybernetics*, 9, p.62-66. https://doi.org/10.1109/TSMC.1979.4310076.

[32] Lloyd, S., **1982**. Least squares quantization in PCM. *IEEE Transactions on Information Theory*, 28, p.129-137. https://doi.org/10.1109/TIT.1982.1056489.

[33] Canny, J., **1986**. A computational approach to edge detection. *IEEE Transactions on Pattern Analysis and Machine Intelligence*, PAMI-8, p.679-698. https://doi.org/10.1109/TPAMI.1986.4767851.

[34] Swain, M. J.; Ballard, D. H., **1991**. Color indexing. *International Journal of Computer Vision*, 7, p.11-32. https://doi.org/10.1007/BF00130487.

[35] Haralick, R. M.; Shanmugam, K.; Dinstein, I., **1973**. Textural features for image classification. *IEEE Transactions on Systems, Man, and Cybernetics*, SMC-3, p.610-621. https://doi.org/10.1109/TSMC.1973.4309314.

[36] Cortes, C.; Vapnik, V., **1995**. Support-vector networks. *Machine Learning*, 20, p.273-297. https://doi.org/10.1007/BF00994018.

[37] Rumelhart, D. E.; Hinton, G. E.; Williams, R. J., **1986**. Learning representations by back-propagating errors. *Nature*, 323, p.533-536. https://doi.org/10.1038/323533a0.

[38] Cover, T.; Hart, P., **1967**. Nearest neighbor pattern classification. *IEEE Transactions on Information Theory*, 13, p.21-27. https://doi.org/10.1109/TIT.1967.1053964.

[39] Hand, D. J.; Yu, K., **2001**. Idiot's Bayes---not so stupid after all?. *International Statistical Review*, 69, p.385-398. https://doi.org/bs2h76.

[40] Sokolova, M.; Lapalme, G., **2009**. A systematic analysis of performance measures for classification tasks. *Information Processing & Management*, 45, p.427-437. https://doi.org/10.1016/j.ipm.2009.03.002.

ARISTON PUBLICATIONS

© Ariston Publications 2026. All rights reserved.